This paper is published as part of a PCCP Themed Issue on:
Electronic Structures and Reaction Dynamics of Open-shell Species

Guest Editors:
Jingsong Zhang - *University of California, Riverside*
Martin Head-Gordon - *University of California, Berkeley*

Editorial

Communication

Papers

Quasiclassical trajectory calculations of the HO_2 + NO reaction on a global potential energy surface

Chao Chen, Benjamin C. Shepler, Bastiaan J. Braams and Joel M. Bowman*

Received 24th December 2008, Accepted 19th March 2009
First published as an Advance Article on the web 2nd June 2009
DOI: 10.1039/b823031e

We report quasiclassical trajectory calculations of the HO_2 + NO reaction using a new full dimensional, singlet potential energy surface (PES) which is a fit to more than 67 000 energies obtained with density functional theory-B3LYP/6-311G(d,p)-calculations. The PES is invariant with respect to permutation of like nuclei and describes all isomers of HOONO, $HONO_2$, saddle points connecting them and the OH + NO_2, HO_2 + NO channels. Quasiclassical trajectory calculations of cross-sections for the HO_2 + NO to form HOONO, $HONO_2$ and OH + NO_2 are done using this PES, for reactants in the ground vibrational state and rotational states sampled from a 300 K Boltzmann distribution. Trajectory calculations illustrate the pathway that HO_2 + NO takes to the energized HOONO complex, which dissociates to products OH + NO_2, reactants HO_2 + NO, or isomerizes to $HONO_2$. The association cross sections are used to obtain rate constants for formation of HOONO and $HONO_2$ in the high-pressure limit, and formation of products OH + NO_2 in the low-pressure limit.

1. Introduction

The reaction

$$HO_2 + NO \rightarrow OH + NO_2 \qquad (R1)$$

plays an important role in catalytic cycles to produce ozone in the upper and lower atmospheres.[1–8] Howard and Evenson[3] carried out the first direct measurement of the rate constant of reaction (R1) using laser magnetic resonance to detect HO_2, OH and NO_2 species at 296 K and a pressure of 140–220 Pa (1.1–1.7 Torr). Subsequently, Howard[4] extended the temperature range from 232 to 403 K and reported a small negative temperature dependence of the rate constant. Imamura and Washida[5] determined the rate constant at 299 ± 2 K by time-resolved photoionization mass spectrometry. Seeley *et al.*[6] measured the rate constant between 206 and 295 K using the turbulent flow technique and also found the reaction to be independent of the pressure between 70 and 190 Torr of N_2. Bohn and Zetzsch[7] increased the pressure of N_2 up to 100 kPa covering the entire tropospheric pressure range at room temperature and also reported no pressure dependence of the rate constant. Following a suggestion from previous work, Bardwell *et al.*[8] extended the temperature range over 183 and 300 K and the pressure range from 75 to 220 Torr. The rate constants were fitted to an Arrhenius form as $3.98^{+0.29}_{-0.27} \times 10^{-12}$ exp[(223 ± 16.5)/T] cm^3 molecule^{-1} s^{-1}, getting good agreement with previous reports of the rate constant, and they also stated the rate constant is invariant with pressure. Thus most experiments reach the conclusions of absence of a pressure dependency and perhaps a slight negative temperature dependency, which indicates that reaction R1 proceeds through a short-lived energized transient complex, which was suggested to be HOONO.[4]

At high-pressure the reaction intermediates $HONO_2$ and in principle HOONO can be formed by a stabilizing collision with a third body,

$$HO_2 + NO + M \rightarrow HONO_2 + M \qquad (R2)$$

$$HO_2 + NO + M \rightarrow HOONO + M \qquad (R3)$$

The more stable product $HONO_2$ was detected in experiments reported by Butkovskaya *et al.*[9,10]

Extensive modeling of reactions (R1)–(R3) has been reported. Sumathi and Peyerimhoff[11] performed an *ab initio* study of the reaction, locating various stationary points including HOONO, and presented the possible pathway to OH + NO_2 and $HONO_2$ formation. Zhu and Lin[12] characterized many minima and saddle points relevant to these reactions as well as the reverse reaction OH + NO_2 using sophisticated *ab initio* methodology. They performed variational transition state theory/RRKM calculations also considering the multi-well coupling to obtain rate constants for reactions (R1)–(R3) and analogous ones for the reverse reaction. Zhang and Donahue[13] modeled the mechanism and kinetics of HO_2 + NO using the multiple-well master equation using a model potential energy surface.

We recently reported a realistic global potential energy surface (PES) for the singlet OH + NO_2 reaction that contains all of the intermediates and saddle points connecting them.[14] Quasiclassical trajectory (QCT) calculations were performed on that PES with a focus on the association products HOONO and $HONO_2$. That PES does describe the products HO_2 + NO, however, not to a level of accuracy that would permit a realistic study of the reaction (R1)–(R3). Here we report a new global PES that does describe the HO_2 + NO channel realistically as well as all the intermediates and the OH + NO_2

Department of Chemistry and Cherry L. Emerson Center for Scientific Computation, Emory University, GA 30322, Atlanta, USA. E-mail: jmbowma@emory.edu

channel. We perform quasiclassical trajectory calculations for the HO_2 + NO reactions using this new PES.

In the next section we briefly describe the construction of the new PES and give some relevant properties of it. In section III we present the details and results of QCT calculations using this PES. These include association cross sections to form OH + NO_2, HOONO, and $HONO_2$, lifetime information of HOONO, and the rate constants of $HONO_2$ and HOONO complex in the high-pressure limit as well as rate constant of OH + NO_2 product in the low-pressure limit. A summary and conclusion are given in section IV.

II. Potential energy surface

The construction of the singlet PES employs procedures developed in our group,[15–17] which produces global fits to data sets of the order of 10^4 electronic energies. The fits are manifestly invariant with respect to permutation of like atoms. As noted, we reported such a PES describing the OH + NO_2 reaction,[14] with a focus on formation of the HOONO/$HONO_2$ complexes. The HO_2 + NO channel was not described accurately and so that PES could not be used in the present study. Thus we supplemented the previous database of 55 471 electronic energies, obtained with density functional theory/B3LYP/6-311G(d,p) calculations, with 11 448 additional energies mostly in the HO_2 + NO region but also in the saddle point regions from HOONO isomers to $HONO_2$. The latest PES is expressed in terms of permutationally invariant polynomials of Morse-type variables y_{ij} given by $y_{ij} = \exp(-r_{ij}/\lambda)$, where r_{ij} is the internuclear distance between nuclei i and j. The RMS fitting error is 0.62 kcal mol^{-1} for energies up to 63 kcal mol^{-1}, relative to the global minimum, a little bit larger than the previous one due in part to the addition of more high-energy data.

The energies of the numerous stationary points, *i.e.*, minima and saddle-point transition states (TS) are shown in Fig. 1. For clarity only minima and saddle points of complexes are connected by dashed lines. From elementary considerations (and confirmed, see below) the expectation is that the HO_2 + NO

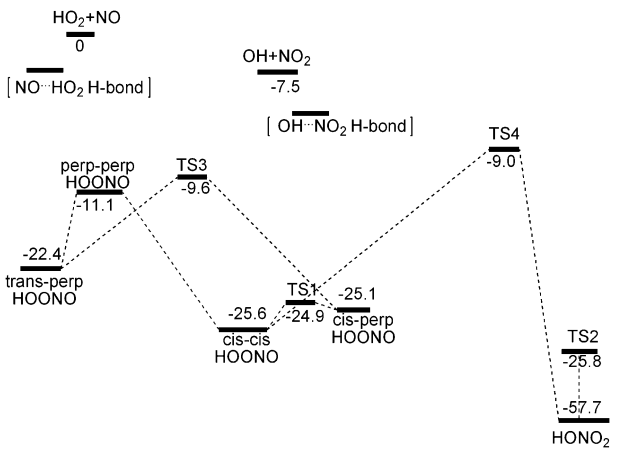

Fig. 1 Energies (kcal mol^{-1}) of indicated minima and transition-state (TS) saddle points of the potential energy surface. The energies of the fragments are also given and the H-bond complexes associated with the fragments are indicated schematically.

Table 1 Comparison of single point energies (kcal mol^{-1}) for the stationary points on the surface relative to the HO_2 + NO minimum

	PES	CCSD(T)/CBS[a]	B3LYP/6-311G(d,p)
HO_2 + NO	0	0	0
OH + NO_2	−7.5	−7	−6.4
$HONO_2$	−57.6	−57.4	−56.6
cis-cis	−25.6	−30.6	−24.7
Cis-perp	−25.2		−23.5
Trans-perp	−22.3		−21.1
Perp-perp	−11.1		−9.6
TS1	−24.9		−23.5
TS2	−25.8		−25.7
TS3	−9.6		−8.9
TS4	−9	−7.2	
H-bond I	−5.3		−2.6
H-bond II	−3.9		−6.5

[a] Ref. 20.

reactants form HOONO isomers *via* simple addition and that formation of nitric acid occurs from isomerization of HOONO. Hydrogen bonding in HO_2 + NO is certainly expected as such bonding has been reported for other reactions involving HO_2, such as HO_2 + H_2O.[18] Indeed two H-bonded complexes have been located at the level of B3LYP/6-311G(d,p) for the singlet state. The geometries and energies are described reasonably by the PES; the comparison of the energies of these two H-bonded complexes is given in Table 1. H-bond complexes also exist for OH + NO_2 and these are also indicated schematically in the figure. These complexes were reported previously,[19] and also discussed in detail in our earlier paper.[14] In that work those complexes were shown to be important in "steering" the reactants to either HOONO or $HONO_2$ and so we made a major effort to verify the accuracy of the PES by doing separate CASPT2 calculations of them.[14] For the present HO_2 + NO reaction these H-bond complexes do not play such a "steering" role since, as mentioned above and shown below, HOONO is always the complex formed from these reactants and/or their associated H-bond complexes. The accuracy of the PES energies is seen in Table 1, which contains a comparison of these energies with previous high-level calculations.[20] For reference, the B3LYP/6-311G(d,p) energies are also given. Other characteristics of the new PES such as the geometry and harmonic frequencies of the stationary points are quite similar to the previous PES which were given in detail and also detailed comparisons with previous high-level *ab initio* calculations showed good

Table 2 For HO_2 + NO reaction, high-pressure limit rate constants of complex HOONO and $HONO_2$, and low-pressure limit rate constants of product OH + NO_2 compared with previous results at 300 K

	300 K		
	Product	Complex	
Rate constant/ 10^{-12} × cm^3 s^{-1}	OH + NO_2	$HONO_2$	HOONO
Calculated[a]	5.5	0.014	14.0
Ref. 4	7.9 ± 1.0		
Ref. 5	6.5 ± 2.0		
Ref. 6	8.0 ± 0.5		
Ref. 7	9.6 ± 1.5		
Ref. 9		0.016 ± 0.005	

[a] Eqn (1) multiplied by the factor $1/Q_{elec}(T)$ described in the text.

agreement.[14] The current PES and the previous one smoothly and realistically interpolate between the open-shell fragments OH + NO_2 and HO_2 + NO and the complex region. (The problems associated with a single reference method applied to a singlet state that dissociates to open shell products are well known and were discussed previously[14] and so we don't repeat that discussion here.) This was verified by doing CASPT2 calculations along one-dimensional cuts starting from the PES optimized HOONO stationary points and separating to the fragments with all other degrees of freedom fixed. The comparisons for cuts leading to HO_2 + NO and OH + NO_2 are shown in Fig. 2 and 3, respectively. As seen, the PES faithfully reproduces the CASPT2 energies. It is interesting to note at the CASPT2/cc-pVTZ level of theory there is a small barrier (0.3 kcal mol^{-1}) in the cut depicting the break-up of *cis–cis* HOONO to HO_2 + NO resulting from an avoided crossing with an excited electronic state.

III. Quasiclassical trajectory calculations of HO_2 + NO reaction

Standard QCT calculations[21] using the new PES were done from 0.12 to 2.4 kcal mol^{-1} initial relative collision energy to determine the cross sections and details of the dynamics to form HOONO, $HONO_2$ complexes and OH + NO_2 product from HO_2 + NO reactants in the ground vibrational states with rotational states sampled from a 300 K Boltzmann distribution. In brief, a normal-mode analysis was done for the HO_2 and NO reactants and they were each given harmonic zero-point energy. Then random sampling was done from each normal mode in the usual fashion. Adjustments were then made to the momenta by adding thermally averaged rotational energy as described elsewhere.[21] The initial separation of the reactants was 20 a_0. The trajectories were propagated with a time-step of 3 atomic units (roughly 0.07 fs) up to 14 ps (200 000 time steps) using the Verlet method. The total energy is conserved to within 0.01 kcal mol^{-1} or less. First, trajectories were performed to determine the maximum impact parameter to within 0.1 a_0. As described in detail below, the formation of the HOONO intermediate is the key process for the formation of both $HONO_2$ and the products OH + NO_2. We found no trajectories in the collision energy considered that make these products without first forming HOONO and so the relevant b_{max} is the one for formation of HOONO. At each collision energy a total of 10 000 trajectories were run by the usual random sampling[21] of b from 0 to b_{max}. We determined that the cross sections reported below are converged to within plus or minus 10% based on considering a fewer number of trajectories to obtain cross sections and also based on our previous studies of the NO_2 + OH reaction.[14]

For each trajectory the time dependence of the distance between the centers of mass of HO_2 and NO, denoted R(t), is

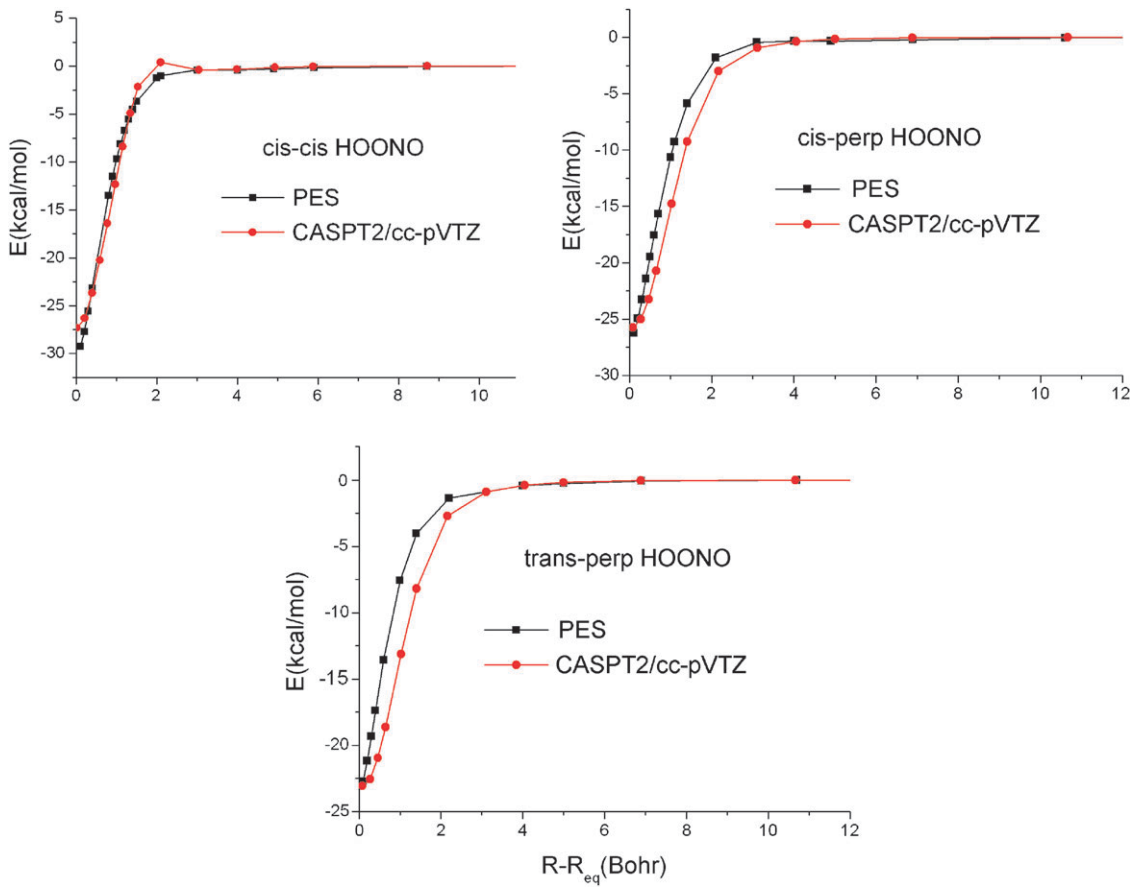

Fig. 2 Comparison of cuts connecting indicated minima to HO_2 + NO obtained directly from CASPT2/cc-pVTZ calculations and the potential energy surface.

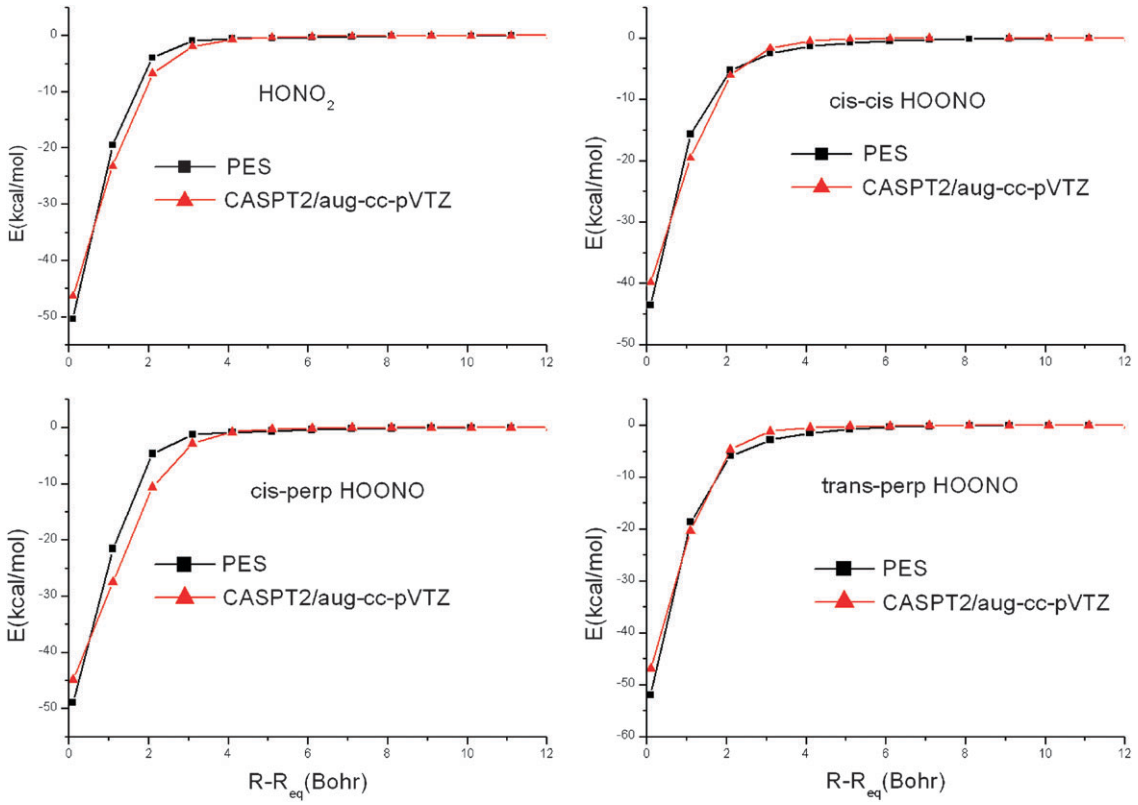

Fig. 3 Comparison of cuts connecting indicated minima to OH + NO_2 obtained directly from CASPT2/aug-cc-pVTZ calculations and the potential energy surface.

used to monitor complex formation. At least one oscillation in $R(t)$ must occur to characterize a trajectory as complex forming. Typically many such oscillations occur and then inspection of the geometry of the complex allows us to identify it. Of course, more than one complex can form along a trajectory and so the characterization of complexes occurs throughout the course of a trajectory. This can in principle lead to a possibly complicated time history if there is rapid isomerization among complexes. This does occur, but only for the isomers of HOONO.

Fig. 4 shows $R(t)$ for two trajectories. In both trajectories, H-bond complexes initially form and go on to form HOONO which in the vast majority of cases goes on to directly form OH + NO_2, as indicated in panel (a). Panel (b) shows a rare trajectory that forms $HONO_2$ *via* isomerization of HOONO and which subsequently leads to the products OH + NO_2. We did not find any trajectories that lead to OH + NO_2 without first forming HOONO. We also find no trajectories leading directly to $HONO_2$. We see facile isomerization among the HOONO isomers but very little isomerization between $HONO_2$ and HOONO. Animation of the trajectories shows that the HOONO/$HONO_2$ isomerization is accomplished by a mechanism in which HOONO begins to dissociate to OH + NO_2, but undergoes a change in relative velocity where the OH rotates causing the incipient fragments to return to form the stable $HONO_2$ complex.

The energy dependence of the total cross sections to form HOONO, $HONO_2$ complexes is plotted in Fig. 5. As seen, the cross section to form $HONO_2$ is very small and within the uncertainties essentially independent of the collision energies. This small cross section is just the result of the low probability of isomerization between HOONO and $HONO_2$, as already noted. The HOONO cross section exhibits a typical E_{coll}^{-q} ($q > 0$) energy dependence.

As noted already, all products of these reactions originate from the HOONO complexes. Thus the total cross section to form HOONO complex, shown in Fig. 5, can be decomposed into cross section to form OH + NO_2, HO_2 + NO and undissociated HOONO up to 14 ps. These are shown in Fig. 6. As seen the cross sections for the HOONO complex to decay into OH + NO_2 and HO_2 + NO are comparable and except at the lowest collision energies the sum of those cross sections is very close to the HOONO cross section. At lower energies the fraction of undissociated HOONO (after 14 ps) is relatively large, as expected, and so the cross section for undissociated HOONO is largest at the lowest collision energy and rapidly drops to zero at roughly E_{coll} of 1.0 kcal mol^{-1}.

The cross sections shown in Fig. 6 were used to obtain estimates of the high-pressure limit rate constants for complex HOONO, $HONO_2$, and the rate constant for product OH + NO_2, in principle in the low-pressure limit. The rate constants were obtained as usual from the expression

$$k(T) = \left(\frac{8}{\pi\mu}\right)^{1/2} \frac{1}{(k_B T)^{3/2}} \int_0^\infty Q_R(E_{coll}) E_{coll} e^{-E_{coll}/k_B T} \, dE_{coll}. \quad (1)$$

We compare our results with various experimental results shown in Table 2. Note the results in that Table include the

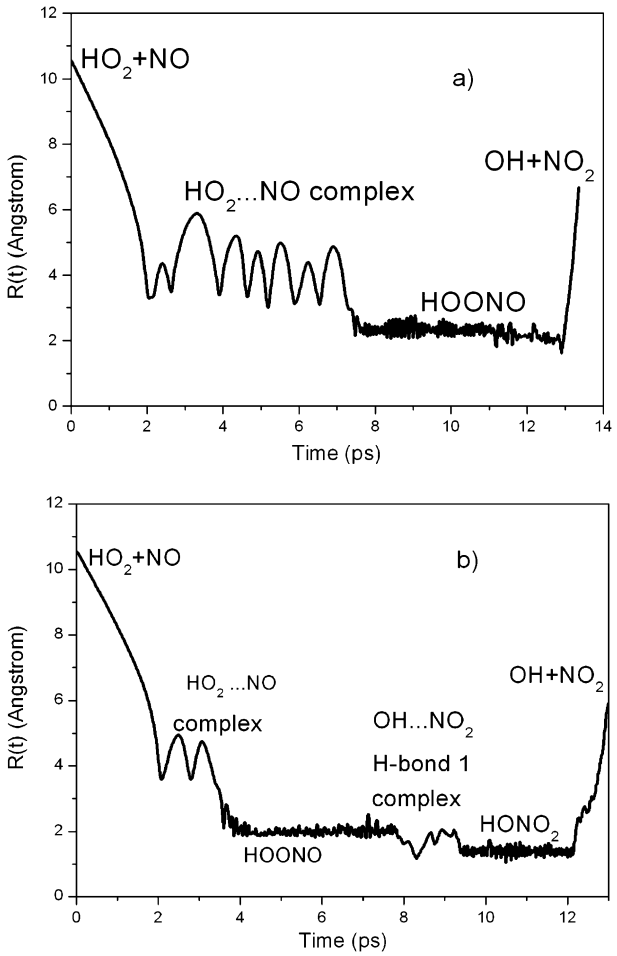

Fig. 4 Time evolution of the distance between the OH and NO_2 centers of mass for a trajectory (a) OH + NO_2 (b) $HONO_2$ isomerization that illustrate a typical pathway to decay to OH + NO_2 and $HONO_2$ formation.

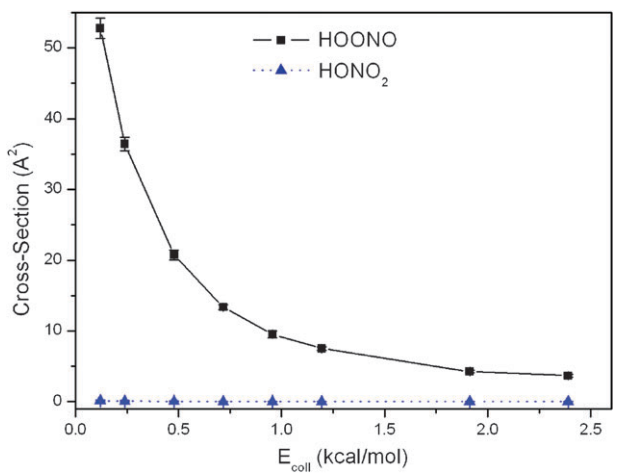

Fig. 5 Association cross-section for HOONO (all isomers) and $HONO_2$ as a function of the initial relative collision energy for the HO + NO_2 reaction.

factor $1/Q_{elec}(T)$, where $Q_{elec}(T)$ is the electronic partition function. This partition function is exactly analogous to the one discussed in detail previously for the HO_2 + OH reaction[22] and is given for the present reaction explicitly by $2[2 + 2\exp(-171/T)]$ where the exponential factor comes from consideration of the difference in energy of the two spin–orbit states of NO.[23] As seen there is very good agreement with experiment for the OH + NO_2 reaction. As noted in the Introduction very little, if any, pressure dependence has been observed for this reaction and while we have not directly addressed this here, the observation is certainly consistent with the present finding of a relatively short-lived HOONO complex, which as noted is the precursor to the OH + NO_2 products. Also our estimate of the high-pressure limit for formation of nitric acid agrees well with the one reported measurement, probably fortuitously so given the small number of trajectories that lead to $HONO_2$. The high-pressure limit rate constant for HOONO is, as expected, much larger than for nitric acid; however, the lifetime is much shorter and so it isn't clear what pressure would actually correspond the "high pressure" without further modeling, which is beyond the scope of this paper.

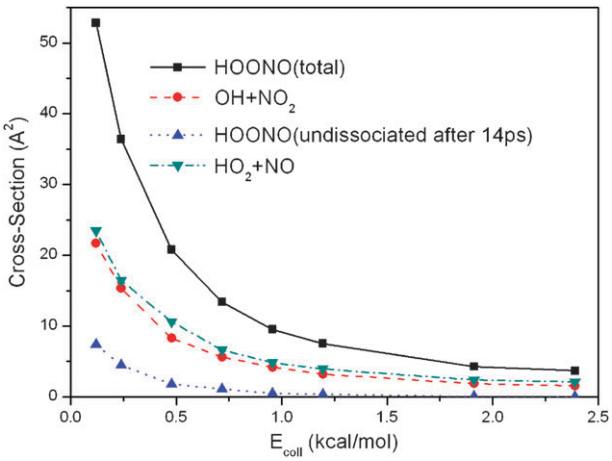

Fig. 6 Collision energy dependence of the total cross section to form HOONO (up to 14 ps) and its reactive (OH + NO_2) and non-reactive (HO_2 + NO) component cross sections as defined in the text.

V. Summary and conclusions

We reported a DFT B3LYP/6-311G(d,p)-based global potential energy surface in full dimensionality for the HO_2 + NO reaction, which describes $HONO_2$, HOONO, OH + NO_2 and HO_2 + NO regions. The PES is invariant with respect to permutation of like nuclei, which is essential for a realistic description of the dynamics of this system. Quasiclassical trajectory calculations were performed to describe the reaction of HO_2 and NO in their ground vibrational states with rotations sampled from a 300 K distribution and with collisional energies from 0.12 to 2.4 kcal mol^{-1}. The total cross section for formation of HOONO (all isomers), $HONO_2$ and OH + NO_2 was presented. HOONO was shown to be the key intermediate to further decay to OH + NO_2, with a nearly equal rate to decay back to HO_2 + NO. After 14 ps, basically all HOONO dissociates at high collision energy. Very little isomerization to $HONO_2$ is observed resulting in a low yield of

$HONO_2$, consistent with experimental observation. Association rate constants in the high-pressure limit for HOONO and $HONO_2$ complex formation, and rate constant for product HO_2 + NO in the low-pressure limit were calculated based on the energy dependence of the cross section, and both agree very well with experimental results.

Acknowledgements

Financial support from the Department of Energy (DE-FG02-97ER14782) and the Office of Naval Research (N00014-05-1-0460) is gratefully acknowledged.

References

1 P. J. Crutzen, *Physics and Chemistry of the Upper Atmosphere*, ed. B. McCormac, D. Reidel, Dordrecht, the Netherlands, 1973, p. 110.
2 W. Chameides and J. C. G. Walker, *J. Geophys. Res.*, 1973, **78**, 8751.
3 C. J. Howard and K. M. Evenson, *Geophys. Res. Lett.*, 1977, **4**, 437.
4 C. J. Howard, *J. Chem. Phys.*, 1979, **71**, 2352.
5 T. Imamura and N. Washida, *Laser Chem.*, 1994, **16**, 43.
6 J. V. Seeley, R. F. Meads, M. J. Elrod and M. J. Molina, *J. Phys. Chem.*, 1996, **100**, 4026.
7 B. Bohn and C. Zetzsch, *J. Phys. Chem. A*, 1997, **101**, 1488.
8 M. W. Bardwell, A. Bacak, M. T. Raventos, C. J. Percival, G. Sanchez-Reyna and D. E. Shallcross, *Phys. Chem. Chem. Phys.*, 2003, **5**, 2381.
9 N. I. Butkovskaya, A. Kukui, N. Pouvesle and G. Le Bras, *J. Phys. Chem. A*, 2005, **109**, 6509.
10 N. I. Butkovskaya, A. Kukui and G. Le Bras, *J. Phys. Chem. A*, 2007, **111**, 9047.
11 R. Sumathi and S. D. Peyerimhoff, *J. Chem. Phys.*, 1997, **107**, 1872.
12 R. S. Zhu and M. C. Lin, *J. Chem. Phys.*, 2003, **119**, 10667.
13 J. Zhang and N. M. Donahue, *J. Phys. Chem. A*, 2006, **110**, 6898.
14 C. Chen, B. C. Shepler, B. J. Braams and J. M. Bowman, *J. Chem. Phys.*, 2007, **127**, 104310.
15 A. Brown, B. J. Braams, K. Christoffel, Z. Jin and J. M. Bowman, *J. Chem. Phys.*, 2003, **119**, 8790.
16 X. Huang, B. J. Braams and J. M. Bowman, *J. Chem. Phys.*, 2005, **122**, 044308.
17 Z. Xie, B. J. Braams and J. M. Bowman, *J. Chem. Phys.*, 2005, **122**, 224307.
18 S. Aloisio and J. S. Francisco, *J. Phys. Chem. A*, 1998, **102**, 1899.
19 K. N. Houk, K. R. Condroski and W. A. Pryor, *J. Am. Chem. Soc.*, 1996, **118**, 13002.
20 D. A. Dixon, D. Feller, C. Zhan and J. S. Francisco, *J. Phys. Chem. A*, 2002, **106**, 3191.
21 W. L. Hase, *Classical Trajectory Simulations*, in *Encyclopedia of Mass Spectrometry*, vol 5, Chemsity and Physics of Gas-Phase Ions, ed. M. Cross and R. Capriolli, Elsevier Science, New York.
22 C. Gonzalez, J. Theisen, L. Zhu, H. B. Schlegel, W. L. Hase and E. W. Kaiser, *J. Phys. Chem.*, 1991, **95**, 6784.
23 NIST Standard Reference Database Number 69, June 2005 Release, http://webbook.nist.gov/chemistry/.